Accepted Manuscript

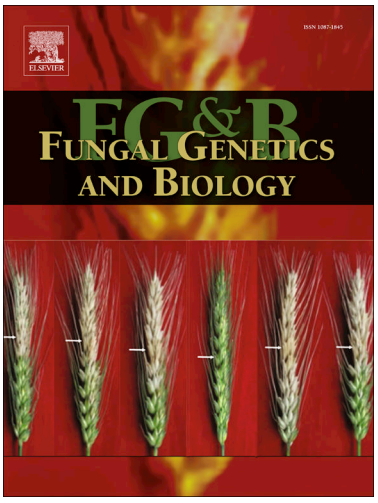

COPI localizes to the early Golgi in *Aspergillus nidulans*

Miguel Hernández-González, Ignacio Bravo-Plaza, Vivian de los Ríos, Mario Pinar, Areti Pantazopoulou, Miguel A. Peñalva

PII: S1087-1845(18)30274-3
DOI: https://doi.org/10.1016/j.fgb.2018.12.003
Reference: YFGBI 3172

To appear in: *Fungal Genetics and Biology*

Received Date: 26 November 2018
Revised Date: 7 December 2018
Accepted Date: 8 December 2018

Please cite this article as: Hernández-González, M., Bravo-Plaza, I., de los Ríos, V., Pinar, M., Pantazopoulou, A., Peñalva, M.A., COPI localizes to the early Golgi in *Aspergillus nidulans*, *Fungal Genetics and Biology* (2018), doi: https://doi.org/10.1016/j.fgb.2018.12.003

This is a PDF file of an unedited manuscript that has been accepted for publication. As a service to our customers we are providing this early version of the manuscript. The manuscript will undergo copyediting, typesetting, and review of the resulting proof before it is published in its final form. Please note that during the production process errors may be discovered which could affect the content, and all legal disclaimers that apply to the journal pertain.

ACCEPTED MANUSCRIPT

COPI localizes to the early Golgi in *Aspergillus nidulans*

by

Miguel Hernández-González[1, 2], Ignacio Bravo-Plaza[1], Vivian de los Ríos[3], Mario Pinar[1], Areti Pantazopoulou[1,4] and Miguel A. Peñalva[1]

1. Department of Cellular and Molecular Biology, Centro de Investigaciones Biológicas CSIC, Ramiro de Maeztu 9, Madrid 28040, Spain

2. Present address: Centre for Mechanochemical Cell Biology, Gibbet Hill Road, Warwick Medical School, University of Warwick, Coventry CV4 7AL, UK

3. Proteomics and Genomics Facility, Centro de Investigaciones Biológicas CSIC, Ramiro de Maeztu 9, Madrid 28040, Spain

4. Present address, Department of Molecular Genetics and Cell Biology, Biological Sciences Division, The University of Chicago

Corresponding authors: Miguel A. Peñalva at penalva@cib.csic.es and Areti Pantazopoulou at apantazopoulou@uchicago.edu

Keywords: Golgi; intracellular traffic; coatomer-I; polarity; exocytosis

Highlights:

- ✓ Coatomer-I (COPI) localizes to the early Golgi (EG)
- ✓ Inactivation of HypB^{Sec7} in the TGN does not delocalize COPI from Golgi cisternae
- ✓ *copA1ts* (*sod^{VI}C*1) maps to ε-COP-binding Carboxyl-Terminal-Domain of α-COP

ACCEPTED MANUSCRIPT

Summary

Coatomer-I (COPI) is a heteromeric protein coat that facilitates the budding of membranous carriers mediating Golgi-to-ER and intra-Golgi transport. While the structural features of COPI have been thoroughly investigated, its physiological role is insufficiently understood. Here we exploit the amenability of *A. nidulans* for studying intracellular traffic, taking up previous studies by Breakspear et al. (2007) with the α-COP/CopA subunit of COPI. Endogenously tagged α-COP/CopA largely localizes to SedV^{Sed5} syntaxin-containing early Golgi cisterna, and acute inactivation of ER-to-Golgi traffic delocalizes COPI to a haze, consistent with the cisternal maturation model. In contrast, the Golgi localization of COPI is independent of the TGN regulators HypB^{Sec7} and HypA^{Trs120}, implying that COPI budding predominates at the SedV^{Sed5} early Golgi, with lesser contribution of the TGN. This finding agrees with the proposed role of COPI-mediated intra-Golgi retrograde traffic in driving cisternal maturation, which predicts that the capacity of the TGN to generate COPI carriers is low. The COPI early Golgi compartments intimately associates with Sec13-containing ER exit sites. Characterization of the heat-sensitive *copA1ts* (*sod^{VI}C*1) mutation showed that it results in a single residue substitution in the ε-COP-binding Carboxyl-Terminal-Domain of α-COP that likely destabilizes its folding. However, we show that Golgi disorganization by *copA1ts* necessitates > 150 min-long incubation at 42ºC. This weak subcellular phenotype makes it unsuitable for inactivating COPI traffic acutely for microscopy studies, and explains the aneuploidy-stabilizing role of the mutation at subrestrictive temperatures.

ACCEPTED MANUSCRIPT

ACCEPTED MANUSCRIPT

Introduction

In the prevailing model, proteins are transported through the Golgi by cisternal maturation (Glick and Luini, 2011; Glick and Nakano, 2009). According to this model Golgi cisternae originating from coalescence of ER-derived coatomer-II (COPII) vesicles undergo changes in their lipid and protein content (i.e. they mature) as they age, until they reach a compositional stage at which they become competent to tear off exocytic carriers bound for the plasma membrane and endosomes. COPI (coatomer-I)-coated vesicles have been proposed to drive this maturation by transporting Golgi resident proteins retrogradely, from older to younger cisternae (Rabouille and Klumperman, 2005), and recent evidence obtained in *S. cerevisiae* strongly supports this contention (Papanikou et al., 2015). In addition to this proposed role in intra-Golgi transport, retrograde COPI vesicles also mediate the retrieval from the Golgi of ER resident proteins that are incorporated into anterograde COPII vesicles and need to be recycled back to the ER once these vesicles fuse with the Golgi (Barlowe and Miller, 2013). Examples are the transmembrane receptors that sort soluble cargo into COPII buds, many of which are selected into COPI vesicles because they contain short sequence motifs in their cytosolic tails that are recognized by the coatomer-I coat (Barlowe and Miller, 2013; Spang, 2013)

Coatomer-I, recruited to membranes by the ARF1 GTPase, assembles into a polymeric cage that initiates the formation of buds that will eventually be detached as COPI vesicles (Dodonova et al., 2017; Dodonova et al., 2015; Yu et al., 2012) or will be elongated into COPI tubules that connect different membranes (Yang et al., 2011). COPI is a heptameric complex formed by two different layers: a cargo binding subcomplex composed of β, γ, δ and ζ subunits and an outer coat subcomplex containing α, β' and ε subunits (Dodonova et al., 2017).

The non-stacked organization that the Golgi apparatus presents in many ascomycete fungi is experimentally advantageous, as it implies that early and late Golgi cisternae are resolvable by optical microscopy (Pantazopoulou and Peñalva, 2011; Wooding and Pelham, 1998). This was crucial for visualizing the maturation of early Golgi into late Golgi cisternae in *S. cerevisiae* (Losev et al., 2006; Matsuura-Tokita et al., 2006) as well as the maturation of late Golgi cisternae into post-Golgi carriers in *Aspergillus nidulans* (Pantazopoulou et al., 2014). Our group has intensively investigated the

ACCEPTED MANUSCRIPT

physiology of the Golgi apparatus in *A. nidulans* [see (Pantazopoulou, 2016) for a review], converting this fungus in a useful experimental organism to study traffic across this organelle. Previous reports on the localization of the *A. nidulans* coatomer α-COP subunit to Golgi cisternae (Breakspear et al., 2007) and the availability of a conditional mutation in the gene encoding this protein (Lee et al., 2002; Whittaker et al., 1999) prompted us to examine the role of COPI in the organization of the *A. nidulans* Golgi. The gene encoding α-COP was initially identified by the *sod*^{VI}*C*1 *ts* mutation that results in stabilization of chromosome VI disomy at subrestrictive temperature (37ºC)(Upshall and Mortimore, 1984). *sod*^{VI}*C* was subsequently renamed *copA* (Breakspear et al., 2007) and the *sod*^{VI}*C*1 mutation, *copA1* (Pinar et al., 2013b).

Here we use GFP-tagged α-COP to show that COPI predominates in early Golgi cisternae that associate dynamically with ER exit sites. Dissipating the early Golgi after blocking the exit of membranes from the ER delocalizes COPI to a cytosolic haze. In contrast, the cisternal localization of COPI is independent of Sec7, suggesting that there is little COPI budding from the *trans*-Golgi network (TGN). Lastly we characterized molecularly the *copA1ts* missense mutation, which affects an amino acid residue located in the carboxyl-terminal domain of α-COP, and demonstrated that it disorganizes the Golgi only very slowly, making it unsuitable for studies of cisternal maturation.

ACCEPTED MANUSCRIPT

ACCEPTED MANUSCRIPT

Materials and Methods

Aspergillus techniques and strains

Complete medium (MCA) and synthetic complete (SC) medium containing 1% glucose and 5 mM ammonium tartrate as carbon and nitrogen source, respectively (Cove, 1966), were used for strain maintenance and conidiospore production. Strains are detailed in Table I. Strains MAD (Madrid) 3822 and 4503 have been deposited in the Fungal Genetics Stock Centre (Kansas State University, Manhattan, KS 66506).

Assembly of endogenously-tagged *copA* genes

DNA molecules used to replace the resident *copA* gene by transgenes encoding C-terminally tagged versions (with GFP and S-tag) were assembled by fusion PCR. (Szewczyk et al., 2006). The CopA-GFP cassette was assembled from three consecutive DNA fragments. The first, encoding the C-terminal coding region of copA lacking the termination codon, was PCR-amplified from genomic DNA with primers FwJCopA (5'-CGCCGCCATGAGACTAC-3') and MHG_29 (5'-GAGTTGGCTAGGGACATACAACCG-3'). The second, encoding a (Gly-Ala)5 linker followed by the GFP coding region and by the *Aspergillus fumigatus pyrG* gene (*pyrGAf*) was PCR-amplified from plasmid p1439 with primers MHG_30 (5'-GCGGTTGTATGTCCCTAGCCAACTCGGAGCTGGTGCAGGCGCTGGAGCC-3') and MHG_31 (5'-CATAACCCATCACACGTCGTCAGGGGAGTCTGAGAGGAGGCACTGATGCG-3').
The third, encoding 3'-flanking sequence of the copA ORF, was PCR-amplified from genomic DNA using primers MHG_32 (5'-TCCCCTGACGACGTGTGATG-3') and MHG_33 (5'-CGCCGCATGGCGTAACTTG-3'). The assembled PCR fragment was introduced into strain MAD1739 (Table I) by transformation. The correct gene replacement events were identified by diagnostic PCR, using flanking primers MHG_36 (5'-GCCATCCCCAGGGACCTTG-3') and MHG_37 (5'-CAGATGCCGTCTCTGCACTTCC-3'). The *copA*-S-tag cassette was constructed similarly, but in the 'middle' fragment the DNA encoding the (Gly-Ala)5 linker was followed by the sequence encoding the 20-residue long S-tag (Liu et al., 2010), instead of GFP. This cassette was introduced into strain MAD5319 and correct gene-replaced strains confirmed as above.

ACCEPTED MANUSCRIPT

Microscopy and image manipulation

These have been described in detail (Peñalva et al., 2017). Briefly hyphae were cultured in pH 6.8 'watch minimal medium' (WMM) using IBIDI multi-well chambers (IBIDI GmbH, Martinriesd, Germany). Images were acquired with a Leica DMI6000 B inverted microscope driven by Metamorph. The microscope was equipped with a Leica 63x/1.4 N.A. Plan Apochromatic objective, a Hamamatsu ORCA ER digital camera (1344 x 1024 pixels) and Semrock GFP-3035B and TXRED-4040B 'BrightLine' filter cubes. For simultaneous channel acquisition we used a microscope filter cube equipped with Chroma 59022x excitation and 59022bs dichroic filters and a Dual-View beam splitter (Photometrics) equipped with Chroma ET525/50 and ET630/75 emission filters for GFP and mCherry/mRFP channels. Microscopy cultures were usually incubated at 28ºC. When indicated, the incubation temperature was shifted from 28ºC to 37ºC as described (Pinar et al., 2013a). Under these conditions it takes 15-20 min for the culture medium to stabilize at 37ºC. Images were processed with Metamorph 7.7.0 (Molecular Device LLC, San José, CA), converted to 8-bit greyscale or 24-bit RGB and annotated with Corel Draw (Corel, Ottawa, Canada). Z-stacks were deconvolved with Huygens Professional (Scientific Volume Imaging, Hilversum, the Netherlands, EU).

Affinity purification of proteins interacting with CopA-S-tag

We used a modified version of the method reported previously (Liu et al., 2010). For mycelial biomass production of strain MAD6765 expressing CopA-S we used MFA, a rich medium consisting of SC supplemented with 2.5% (v/v) of corn steep liquor syrup (Solulys 048R, Roquette Laisa S.A., Valencia, Spain), 50 mM each of Na_2HPO_4 and NaH_2PO_4, 50 mM NaCl, 3% (w/v) sucrose as main C source, 20 mM $(NH_4)_2SO_4$ as main N source and appropriate additions for the vitamin auxotrophies carried by the strain. Cultures were inoculated with a conidiospore suspension and incubated for 14-15 h at 30ºC with shaking. Mycelia were collected by filtration, washed with distilled water and lyophilized. 1.75 g of lyophilate were transferred to a 50 ml Falcon tube containing ceramic beads (MP Biomedicals, 1/4 inch) and ground to a fine powder with a FastPrep set at power 4 for 20 sec. The powder was resuspended in 45 ml of extraction buffer containing 25 mM HEPES, pH 7.5, 0.5% v/v NP40, 150 mM KCl, 2 mM EDTA, 1 mM DTT, 5 µM MG132, Complete ULTRA EDTA-free protease inhibitor cocktail (Roche) and 5 ml of 0.6 mm glass beads. The resulting suspension was homogenized for 15 sec at maximal power in the FastPrep and subsequent incubation for 10 min at 4ºC in a rotating wheel. This step was repeated two additional times

ACCEPTED MANUSCRIPT

before centrifuging the resulting extract at 15,000 x g for 30 min at 4ºC in a Thermo Scientific F-21 rotor. BSA was added to a final concentration of 1% (w/v) to the approximately 35 ml of recovered supernatant, which was next mixed with 0.5 ml of S-protein agarose (Novagen) equilibrated with extraction buffer containing 1 % BSA. The mixture was incubated for 4 h at 4ºC in a rotating wheel before collecting the agarose beads and bound proteins by centrifugation for 2 min at 1400 rpm and 4ºC in an Eppendorf tabletop centrifuge. The slurry was washed four times for 10 min at 4ºC with 10 ml of ice-cold 'washing buffer' containing 25 mM HEPES pH 7.5, 300 mM KCl, 2 mM EDTA and 1 mM DTT. Lastly the washed slurry was transferred to a 2 ml Eppendorf tube and mixed with 0.5 ml of a 12 mg/ml solution of S-peptide, adjusted to pH 7.5. The tube was incubated for 15 min at 37ºC with mild shaking before collecting the supernatant after centrifugation in a microfuge. This step was repeated a second time. The two eluates were pooled and the recovered proteins were concentrated by precipitation with 10% (v/v) TCA. The protein pellet was resuspended in 100 µl of Laemmli buffer. One third of the material was loaded onto a 10% SDS-polyacrylamide gel that was run until proteins moved ~ 1 cm into the separation gel. Then the portion of the gel containing the protein mixture (identified after staining with colloidal Coomassie) was excised and processed for MS/MS analysis.

LC-MS and MS data analysis

Tryptic peptide identification was carried out using an Easy-nLC 1000 nano-flow chromatograph (Thermo Fisher) coupled to a Q Exactive mass spectrophotometer. Peptide samples (4 µl) were loaded onto an Acclaim PepMap 100 pre-column (Thermo Fisher) connected to a separating RSLC PepMap C18 column (15 cm long, 50 µm inner diameter and 2 µm particle size; Thermo Fisher). The column was run with a flow rate of 300 nL/min, using 0.1% formic acid in water as solvent A and 0.1% formic acid and 100% acetonitrile as solvent B. The gradient profile was set as follows: 0%–35% solvent B for 90 min, 35%-100% solvent B for 4 min, 100% solvent B for 8 min. MS analysis was performed with a Q Exactive mass spectrometer (Thermo Scientific). For ionization, 2000 V of liquid junction voltage and 270ºC capillary temperature were used. The full scan method employed a m/z 400–1500 mass selection, an Orbitrap resolution of 70,000 (at m/z 200), a target automatic gain control value of $3x10^6$, and maximum injection times of 100 ms. After a survey scan, the 15 most intense precursor ions were selected for MS/MS fragmentation, which used a normalized collision energy of 27 eV. MS/MS scans were acquired with a starting mass of m/z 100, automatic gain control target of $2x10^5$, maximum injection time of 100 ms, resolution of 17,500 (at m/z

ACCEPTED MANUSCRIPT

200), intensity threshold of $8x10^3$ and isolation window of 2 m/z units. Charge state screening was enabled to reject unassigned, singly charged, and equal or more than seven protonated ions. A dynamic exclusion time of 20 s was used to discriminate against previously selected ions. MS data were analyzed with Proteome Discoverer 1.4.0.288 software (Thermo Fisher). Mass spectra *.raw files were searched against a modified version of *Aspergillus nidulans* FGSC A4 version_s10m02-r03_orf_trans_all (8223 sequences proteins entries, http://www.aspergillusgenome.org) using MASCOT. Precursor and fragment mass tolerance were set to 10 ppm and 0.02 Da, respectively, allowing 2 missed cleavages, carbamidomethylation of cysteines as a fixed modification and methionine oxidation as a variable modification. Identified peptides were filtered using Percolator (Kall et al., 2007) with a q-value threshold of 0.01.

ACCEPTED MANUSCRIPT

ACCEPTED MANUSCRIPT

Results and discussion

Functional CopA-GFP expressed at physiological levels localizes to Golgi cisternae

A previous study used a strain expressing C-terminally tagged CopA-GFP under the control of the strong *alcA*^{p} promoter to conclude that α-COP localizes to Golgi cisternae (Breakspear et al., 2007). To avoid interference of overexpression we GFP-tagged CopA endogenously. *copA* encoding α-COP is essential (Whittaker et al., 1999). Strains expressing physiological levels of CopA-GFP as the only source of α-COP grew similarly to the wt, indicating that the fusion protein is functional. Like Breakspear et al. (2007), we observed that CopA-GFP localizes to cytosolic punctate structures whose shape and distribution resembled Golgi cisternae labeled with other known early Golgi and TGN residents (Figure 1A)(see below), although the observation that CopA-GFP puncta invade the hyphal tips suggested that these cisternae have early Golgi identity (see below). As also reported (Breakspear et al., 2007), CopA-GFP puncta are polarized, concentrating in the apicalmost 20 μm of the hyphal tip cells (Figure 1A). Addition to liquid microscopy cultures of brefeldin A (BFA), a drug that interferes with the function of ARF1 in the Golgi (Peyroche et al., 1999), results in the rapid aggregation of Golgi cisternae into larger structures (Pantazopoulou and Peñalva, 2009; Pantazopoulou and Peñalva, 2011). CopA-GFP puncta formed these characteristic aggregates with BFA (Figure 1B), indicating that these puncta are indeed Golgi cisternae, and excluding the possibility that they represent ER exit sites (ERES), as these domains of the ER are not affected by BFA (Pantazopoulou and Peñalva, 2009) (see also below).

This observation that CopA does not become cytosolic in the presence of BFA appeared paradoxical, given that COPI is a GTP-ARF1 effector and BFA targets the complexes between GDP-ARF1 and its Sec7 domain-containing GEFs, GeaA^{Gea1} and Sec7 (HypB in *A. nidulans*) (Mossessova et al., 2003; Renault et al., 2003). However, it should be noted that GDP-ARF1 can be recruited to the Golgi before the nucleotide exchange occurs (Gommel et al., 2001) and that BFA inhibits the nucleotide exchange reaction but not the prior formation of the complex(es) between GDP-ARF1 and Sec7/Gea1. The association of these GEFs with GDP-ARF1 promotes a conformation of ARF1 that resembles the GTP conformation in that it allows the insertion of the myrystoylated amphipathic N-terminal helix of ARF1 into membranes, and thus the

ACCEPTED MANUSCRIPT

drug prevents ARF1 membrane attachment only partially (Béraud-Dufour et al., 1999). We speculate that this mode of action combined with the natural resistance of fungi to the drug (a fungal metabolite) (Pantazopoulou and Peñalva, 2009) may lead to partial inhibition of *A. nidulans* ARF1 activity that would underlie the formation of cisternal aggregates and explain the fact that COPI does not become cytosolic.

Other subunits of the COPI coatomer copurify with CopA (α-COP)

To validate the use of CopA as a proxy for COPI we tagged the protein with a C-terminal S-peptide by gene replacement, and used CopA-S as bait for affinity purification. Shotgun analysis of the proteins pulled down by CopA-S-tag (Figure 2) revealed the presence in the affinity purified material of the β' and ε subunits of COPI (i.e. the two other components of the outer coat subcomplex) as well as the βδ half of the adaptor subcomplex, confirming that α-COP can be used to reveal Golgi compartments enriched in COPI. However, the subunits of the γζ half subcomplex (structurally homologue to βδ) were largely substoichiometric in the preparation. This might be explained by the fact that the β subunit links the adaptor and outer-coat layers within the same unit of the coatomer (Dodonova et al., 2017), and thus βδ would be expected to co-purify more tightly with the outer-coat α-subunit than γζ. Alternatively, although the COPI heptamer containing α-COP exists as a single entity in the cytoplasm of mammalian cells (Hara-Kuge et al., 1994), fungal COPI might not exist in the cytosol as a holocomplex and might be assembled on membranes from more than one cytosolic entity. In any case these experiments indicate that the signal of CopA-GFP reflects the subcellular localization of COPI.

CopA-GFP localizes to early Golgi cisternae

To determine where in the Golgi COPI resides we co-filmed CopA-GFP with the mCh-labeled early Golgi syntaxin $SedV^{Sed5}$ (an integral membrane protein) and with the TGN marker $mRFP\text{-}PH^{OSBP}$, which is targeted to the TGN by the concerted action of ARF1 and PtdIns4P (Levine and Munro, 2002). Maximal intensity projections of Z-stacks of simultaneously acquired images in the two channels (with a beam splitter) showed that CopA puncta and TGN cisternae are different structures: CopA puncta are smaller and invade the hyphal tip region, whereas, as reported (Pantazopoulou and Peñalva, 2009), TGN cisternae are scarce in this region. Indeed CopA and TGN puncta did not colocalize (Figure 3A). In contrast, the CopA and $SedV^{Sed5}$ signals overlapped substantially (Figure 3B). Quantitative assessment of this overlap

ACCEPTED MANUSCRIPT

confirmed these conclusions: Pearson's coefficients were, on average, 0.72 ± 0.06 S.D. for CopA and SedV^{Sed5} in *n*= 11 hyphal tip cells and 0.27 ± 0.12 for CopA and PH^{OSBP} in *n* = 13 cells (see Figure 3C for the actual distribution of values). To reinforce the conclusion that CopA preferentially localizes to the early Golgi, we used BFA. Cisternal aggregates induced by BFA maintain distinct early or TGN identity (Pantazopoulou and Peñalva, 2011; Pinar et al., 2013a). BFA-aggregated TGN cisternae did not contain CopA (Figure 3D), whereas BFA-aggregated early Golgi ones did (Figure 3E). These data indicate that CopA predominates in the early Golgi, which concurs with the finding that fluorescently-tagged *S. cerevisiae* COPI subunits colocalize strongly with the Vrg4 GDP-mannose transporter, an early Golgi resident (Papanikou et al., 2015). As COPI vesicles uncoat before fusing with target membranes, the α-COP cisternal signal must reflect their budding. Thus our data indicate that COPI budding takes place mainly from early Golgi (i.e. SedV^{Sed5}) cisternae. Movies constructed with sequential middle planes of a strain expressing mCh-SedV^{Sed5} and CopA-GFP (Supplemental Movie 1) showed that even though the signals of the two fusion proteins substantially correlate, they do not overlap completely, which might suggest that COPI buds from subdomains of the early Golgi cisternae.

We acknowledge that our colocalization data do not rule out the possibility that a minor fraction of COPI vesicles buds from TGN membranes. However, it should be noted that the detectable CopA signal colocalizing with the TGN marker by Pearson's analysis (Figure 3C) could represent cisternae captured in the process of maturation. In this regard, time-lapse movies of middle planes (Supplemental Movie 2) of a strain co-expressing CopA-GFP and mRFP-PH^{OSBP} showed that COPI structures not only are often seen in close dynamic association with TGN cisternae but in some cases overlap with the TGN signal.

α-COP relocalizes to the cytosol if the biogenesis of the Golgi is impaired

The Golgi is a dynamic organelle made up of membrane-bound cisternae that originate from COPII-coated vesicles derived from the ER. The biogenesis of these vesicles is governed by the GTPase SAR1 [SarA^{Sar1} in *A. nidulans* (Hernández-González et al., 2014)]. Using the *ts* allele *sarA6* we have previously demonstrated that impairment of SarA^{Sar1} by shifting cells from permissive (28ºC) to restrictive (37ºC) conditions on the microscope stage results in the rapid relocalization of early Golgi transmembrane proteins into the ER and the somewhat slower delocalization of TGN

ACCEPTED MANUSCRIPT

markers to the cytosol, in agreement with the prediction of the cisternal maturation model that cisternae are not stable entities (Hernández-González et al., 2014). Figure 4 shows that upon temperature up-shift *sarA6* results in the rapid delocalization of CopA-GFP from Golgi cisternae to a cytosolic haze. Thus, if the biogenesis of the Golgi is impaired α-COP disperses, which is consistent with the fact that COPI vesicles bud from Golgi cisternae.

Relationship between COPI-budding Golgi cisternae and ERES

To investigate the spatiotemporal relationship between the specialized export regions of the ER (ER exit sites, ERES) (Sprangers and Rabouille, 2015) and the early Golgi compartments that generate COPI traffic, we co-filmed GFP-CopA with mCh-Sec13. Sec13 is a component of the outer coat layer of COPII vesicles that concentrates on ERES (Rossanese et al., 1999). As previously observed with Sec23-GFP (another component of COPII)(Pantazopoulou and Peñalva, 2009) mCh-Sec13 ERES appear as numerous punctate structures (Figure 5) (Supplemental movie 3 shows a 3D reconstruction —streaking in the lateral view is due to lower optical resolution in the Z-axis). COPI and ERES do not appear to overlap overall, but the respective signals seem to associate closely in some instances (Figure 5). Supplemental Movie 4 (a hyphal tip cell) and Supplemental Movie 5 (a detail of the latter) show the changes in shape that early Golgi cisternae and ERES undergo over time (at a time resolution of 0.5 fps) and reveal transient protrusions that appear to approximate these structures. While these diffraction-limited images/movies have not enough resolution to determine the proximity of the membranes, they should be considered in the context of a recent report concluding that in *S. cerevisiae* ERES and the early Golgi exchange membrane and cargo by a 'hug-and-kiss' mechanism, rather than by vesicular traffic (Kurokawa et al., 2014).

A functional TGN is not required for α-COP recruitment to the early Golgi

COPI is recruited to Golgi membranes by GTP-ARF1. Thus inactivating ARF1 in a compartment that generates COPI vesicles should alter COPI localization. According to the cisternal maturation model an early Golgi cisterna progresses to late (i.e. TGN) identity because its 'early' components are gradually removed away by COPI-mediated traffic. Therefore a mature TGN cisterna would no longer need to generate COPI vesicles once it has acquired its full 'late' identity. Two compartment-specific ARF1 GEFs, Gea1 ($GeaA^{Gea1}$) and Sec7 ($HypB^{Sec7}$), activate ARF1 in the early Golgi and the

ACCEPTED MANUSCRIPT

TGN, respectively (Arst et al., 2014). At 37ºC the *hypB5* ts mutation impairs Sec7, and thus ARF1 function in the TGN, shifting the PtsIns4P- and ARF1-dependent reporter PH^{OSBP} towards the cytosol (Pantazopoulou et al., 2014). However, incubation of mutant *hypB5* cells expressing CopA-GFP at the restrictive temperature did not delocalize COPI from punctate cisternae, even after relatively long (60 min) incubation times (Figure 6), indicating that the activation of ARF1 at the TGN does not crucially contribute to the Golgi localization of COPI.

The *hypA1* ts mutation affects Trs120, a component of the TRAPPII oligomeric complex that acts as GEF for $RabE^{RAB11}$ at the TGN (Pinar et al., 2015). Impairment of TRAPPII by shifting *hypA1* cells to 37ºC prevents the biogenesis of post-Golgi carriers at the TGN (Pinar et al., 2015) without dissipating TGN cisternae (Hernández-González et al., 2018). However, *hypA1* did not delocalize COPI from the Golgi either (Figure 6).

That neither *hypA1* nor *hypB5* precludes the localization of COPI to cisternae indicates that the recruitment of COPI to the Golgi is not dependent on the functional status of the TGN and, more specifically, as experiments with *hypB5* imply, on the activation of ARF1 in the TGN. This is consistent with the above observation that COPI largely localizes at the $SedV^{Sed5}$ early Golgi (Figure 3), where its recruitment by ARF1 would be governed by the early Golgi-specific GEF, $GeaA^{Gea1}$, which has been shown to colocalize with $SedV^{Sed5}$ (Arst et al., 2014). Therefore, our data suggest that the capacity of TGN cisternae to generate COPI vesicles is low, as predicted by the cisternal maturation model. The TGN delivers AP-1/clathrin coated vesicles bound for the endosomes (Daboussi et al., 2012; Schultzhaus et al., 2017). In *Aspergillus nidulans* AP-1-mediated regulation of traffic connecting the endosomes, the TGN and the plasma membrane is required for polarized growth (Martzoukou et al., 2018). COPI and AP-1/clathrin are ARF1 effectors, thus perhaps the low capacity of the TGN to generate COPI traffic ensures that its exit routes are kept expedite by 'reserving' activated ARF1 to recruit AP-1. Work with *S. cerevisiae* has shown that the acute inactivation of COPI extends the lifespan of early Golgi cisternae, generating a sort of hybrid structure on which the TGN marker Sec7 cycles normally (Papanikou et al., 2015), which strongly indicates that COPI is required to withdraw early identity membranes from early-to-late maturing cisternae, but is dispensable for late Golgi protein homeostasis.

ACCEPTED MANUSCRIPT

Our definition of the early Golgi is based on its content of SedV^{Sed5} (syntaxin-5) (López-Berges et al., 2016; Pantazopoulou and Peñalva, 2011; Pinar et al., 2013a). However, the early Golgi may not be functionally homogeneous, as indicated by Glick and co-workers (Day et al., 2013), who proposed that the early Golgi actually involves two succeeding stages denoted 'cisternal assembly' and 'carbohydrate synthesizing'. According to cisternal maturation, 'carbohydrate synthesizing' cisternae would deliver intra-Golgi COPI retrograde traffic to the younger 'cisternal assembly stage' ones. In addition, it is well established that the early Golgi generates COPI traffic to the ER. This traffic presumably buds from cisternae at the 'cisternal assembly' stage (Papanikou and Glick, 2014). Therefore we interpret that all early Golgi cisternae identified by SedV^{Sed5} bud COPI vesicles, whether destined to the ER or percolating between cisternae of the early Golgi themselves (Papanikou and Glick, 2014).

Molecular characterization of *copA1ts*

The available *ts* mutation *copA1* affecting α-COP (Whittaker et al., 1999) had not yet been characterized. Sequencing revealed that the mutation results in a double AT(3491,3492)GA nucleotide change in the genomic sequence, causing an Ile1048Asp substitution in the 1211 residue long CopA protein [coordinates as in AspGD AN3026, which adds six additional codons/amino acids at the N-terminus to the sequence reported by (Whittaker et al., 1999)]. From N- to C-terminus α-COP is composed of two β-propeller domains, followed by an α-solenoid domain, an unstructured linker and a C-terminal domain (CTD) that binds ε-COP (see Figure 2 scheme). Conserved Ile1048 (Ile1045 in the crystalized yeast protein) lies in the CTD, within a cluster of hydrophobic residues that contribute to the overall fold of the domain (Figure 7A). Thus Ile1048Asp predictably disrupts the folding of the CTD and, consequently, the recruitment of ε-COP to α-COP. It has been proposed that the α-COP CTD/ε-COP heterodimer projects away from the COPI coat to mediate the interaction of the COPI vesicle with the acceptor Dsl1 tethering domain in the ER (Hsia and Hoelz, 2010). However, we note that ε-COP is the only COPI subunit that is not essential in *S. cerevisiae* and that ablation of *A. nidulans* ε-COP does not affect vegetative growth either (Kang et al., 2015), suggesting that the conditionally lethal phenotype of *copA1ts* does not result from its effects on the α-COP CTD/ε-COP heterodimer, but is rather an effect on COPI as a complex.

Subcellular phenotype of *copA1ts*

ACCEPTED MANUSCRIPT

Next we set out to determine the effects on the Golgi of inactivating COPI with *copA1^{ts}*, using wt and mutant strains co-expressing GFP-SedV and mRFP-PH^{OSBP} as early Golgi and TGN reporters, respectively. *copA1^{ts}* colonies grow normally at 25-30ºC and not at all at 42ºC, but the mutation allows substantial growth at 37ºC (Pinar et al., 2013b)(Figure 7B). This compelled us to use 42ºC to achieve restrictive conditions in microscopy studies, after confirming that when *copA1ts* conidiospores were incubated overnight at 42ºC in microscopy chambers they did not progress beyond a swollen cell stage (Figure 7C), which indicated that also at the cellular level the mutation is completely restrictive at 42ºC.

We precultured *copA1ts* hyphae in microscopy chambers for 18 h at 28ºC and verified that at this temperature the Golgi reporters were not affected by the mutation (Figure 7D). Then we shifted up the temperature to impair COPI function. As our microscope setup cannot be heated above 39ºC, the chambers were transferred from 28ºC to an external incubator set at 42ºC and, after different times of incubation at the latter temperature, returned to the on-stage incubator preheated at 37ºC before rapidly photographing the hyphae. Control experiments showed that the Golgi was not disrupted by this temperature shift in the wild-type (Figure 7D). Somewhat unexpectedly, preliminary experiments demonstrated that incubation at 42ºC up to 45 min did not cause any noticeable effect on the *copA1ts* Golgi either. Subsequent experiments showed that only after 150 min at 42ºC was an effect of *copA1ts* clearly patent. At this time the population consisted of hyphae that had lost Golgi cisternae completely or partially (with remnants of the TGN still visible) (Figure 7E1-E3), and of hyphae in which Golgi structures were still visible but had an abnormal distribution or morphology (Figure 7E4 and E5). Nevertheless the morphologically abnormal tips seen in the majority of hyphae confirmed that under these conditions *copA1ts* causes an exocytic defect affecting cell wall morphogenesis, as reported (Lee et al., 2002).

The phenotypic consequences of mutations affecting α-COP are difficult to anticipate due to the multiple roles that this subunit plays. α-COP N-terminal domains contribute structurally to the outer coatomer layer (Dodonova et al., 2017) and recognize Lys-rich motifs epitopes in retrograde cargo trafficking from the Golgi to the ER (Schroder-Kohne et al., 1998; Spang, 2013). In contrast, the α-COP CTD/ε-COP heterodimer has been proposed to mediate interaction of the coat with the Dsl1 tether (Hsia and Hoelz, 2010). Given the position of Ile1048 in the α-COP CTD and the dispensability of ε-COP, the weak subcellular phenotype of *copA1ts* would be consistent with the mutation affecting the role of the α-COP CTD/ε-COP heterodimer

ACCEPTED MANUSCRIPT

directly and, after long incubation times at 42ºC, the stability/structure/function of α-COP/COPI.

The widely used *S. cerevisiae ret1-1* (G227D) mutation also affecting α-COP is a weak *ts* allele (Eugster et al., 2004; Schroder-Kohne et al., 1998). The phenotypic mildness of this and other extant α-COP mutations has hampered research on the physiological role of COPI in Golgi maturation (Papanikou et al., 2015): for example, the *ret1-1* (α-COP) *ts* mutation slows down but does not arrest cisternal maturation (Matsuura-Tokita et al., 2006), which might have been interpreted as evidence against a direct role of COPI in this process would it not have been for the reported weakness of this allele (Eugster et al., 2004). To settle this issue, Papanikou et al. (2015) used an 'anchor away' method to inactivate COPI acutely, and concluded that strong impairment of coatomer function results in the formation of hybrid early/late Golgi structures, which strongly supports the view that COPI drives maturation of the early Golgi. The fact that we have not visualized these hybrid structures arguably results from the inappropriateness of *copA1ts* to block COPI function acutely.

Lastly we note that our results strongly support the interpretation of Whittaker et al. (1999) that the stabilization of disomy for its chromosome VI observed for *copA1ts* (formerly *sod^{VI}C1)* at 37ºC simply reflects the fact that an increased dosage of the gene compensates the mild growth defect, giving the disomic a selective growth advantage over the eusomic strain.

Acknowledgements

Work supported by MINECO Grants BIO2012-30965 and BIO2015-65090-R and by the Comunidad de Madrid Grant S2017/BMD-3691 "InGEMICS-CM" (with contributions of the European Social Fund and the European Regional Development Fund), to MAP. MH-G and IB_P were holders of a Formación de Personal Investigador (FPI) pre-doctoral contract. MAP is member of the Centro de Investigaciones Biológicas Intramural WhiteBiotech Unit (https://www.cib.csic.es/interdepartmental-unit). We thank Hee-Moon Park (Chungnam National University, Korea) for sharing a *copA1ts* strain and Elena Reoyo and Ana Alonso for technical assistance. The authors do not have any conflict of interest to declare.

ACCEPTED MANUSCRIPT

Legends to Figures

Figure 1. Localization of endogenously tagged CopA-GFP

(A) Maximal intensity projection of a deconvolved Z-stack of a hypha expressing CopA-GFP. The position of two nuclei (nuc1 and nuc2) is indicated. The linescan shows the polarization of the CopA-GFP structures. (B) A hypha of a culture that has been treated for 10 min with BFA. Arrows indicate the characteristic Golgi aggregates

Figure 2. Characterization of proteins co-purifying with S-tagged CopA by LC-MS/MS shotgun proteomics

Proteins associating with CopA-S-tag were recovered from a crude extract by S-protein agarose affinity chromatography. The column eluate was submitted to shotgun proteomic analysis. The table shows the systematic gene numbers of COPI subunits and the number of peptide spectrum matches (PSMs) identified in the eluate for each protein (non-COPI proteins detected in the analysis were omitted for simplicity). PSMs 'mock' denotes the number of PSMs obtained in a 'mock' purification using a protein extract from a strain lacking the S-tagged bait. 'Score' is the number of PSMs/number of amino acids multiplied by 10e3. The drawing shows a highly schematic representation of the components of the COPI coat.

Figure 3. CopA resides on the early Golgi cisternae

(A) Absence of colocalization of CopA-GFP with the TGN marker PH^{OSBP}, tagged with mRFP (B) Colocalization of CopA-GFP with the mCherry-tagged early Golgi t-SNARE $SedV^{Sed5}$. (C) Pearson's coefficients were used to quantitatively estimate the degree of colocalization of each pair of markers in several hyphae. Plots indicate average values with S.D. error bars. The two datasets were significantly different in an unpaired *t*-test with Welch's correction. (D) CopA and PH^{OSBP} re-localize to different Golgi aggregates in cells treated with brefeldin A (BFA). (E) $SedV^{Sed5}$ and CopA colocalize in Golgi aggregates induced by BFA. All images are displayed at the same magnification and represent maximal intensity projections of deconvolved Z-stacks.

Figure 4. COPI delocalizes to a cytosolic haze upon blocking ER exit

Wild-type and *sarA6* cells expressing CopA GFP were shifted from 28ºC to 37ºC in the microscopy stage incubator. Times after the shift is indicated in minutes.

ACCEPTED MANUSCRIPT

Figure 5. Co-imaging of ERES and COPI-containing Golgi membranes

ER exit sites (ERES) were labeled with mCherry-Sec13. Sec13 is a component of the outer layer of the COPII coat. Images were acquired with a beam splitter and displayed as maximal intensity projections of deconvolved Z-stacks.

Figure 6. Mutations impairing TGN regulators do not delocalize COPI from Golgi membranes

Hyphae expressing CopA-GFP were cultured at 28ºC overnight and shifted to 37ºC for 60 min. Photographs were taken before and after the shift. Images are maximal intensity projections of deconvolved Z-stacks. Note the characteristic swelling of the tips in the mutant cells at 37ºC, indicating that exocytosis is impaired and that therefore the mutations have phenotypic consequences.

Figure 7. Characterization of *copA1ts* and its effects on the Golgi

(A) *copA1ts* results in an Ile1048Asp substitution in the CTD domain of α-COP. The left drawing shows the relative position of a cluster of hydrophobic residues containing the equivalent Ile1045 in the CTD domain of *S. cerevisiae* α-COP (pink) bound to the ε-COP subunit (yellow). The drawings were prepared with PyMol using pdb database entry 3mv2 coordinates. Ile1048 belongs to a REYIL/V motif conserved between fungi and humans. Blue amino acid codes indicate conservative substitutions in the *A. nidulans* α-COP CTD compared to the crystallized yeast equivalent. (B) Growth tests of a *copA1ts* strain compared to the wild-type. Plates were incubated for 3 days at 37ºC. Both strains carry a *yA2* mutation resulting in yellow conidiospores. (C) Wild-type and *copA1ts* conidiospores were inoculated in microscopy chambers and incubated overnight at 42ºC. (D) Control experiments showing that the pattern of early Golgi (GFP-SedV) and TGN (mRFP-PH) cisternae is not affected by *copA1ts* at 28ºC, or by shifting wild-type cells to 42ºC for 2.5 h. (E) Effects of *copA1ts* on early Golgi and TGN cisternae after shifting cells from 28ºC to 42ºC for 2.5 h. All images are maximal intensity projections of deconvolved Z-stacks and are shown at the same magnification.

ACCEPTED MANUSCRIPT

Appendix A. Supplementary Materials

Supplemental Movie 1

200 frame-frame-sequence built with middle plane images of mCherry-SedV (early Golgi) and CopA-GFP, simultaneously acquired with a beam splitter. The cell was filmed at 5 fps for a total of 40 s. The movie is accelerated 2 x.

Supplemental Movie 2

150 frame-frame-sequence built with middle plane images of mRFP-PH^{OSBP} (TGN) and CopA-GFP, simultaneously acquired with a beam splitter. The cell was filmed at 4 fps for a total of 37.5 s. The movie is accelerated 3.75 x.

Supplemental Movie 3

3D reconstruction of ER exit sites (ERES) in a cell expressing Sec13-mCherry. It was built with a Z-stack consisting of 25 optical sections acquired with a 0.25 µm Z-pass

Supplemental Movie 4

60 frame-sequence built with middle plane images of Sec13-mCherry and CopA-GFP, simultaneously acquired with a beam splitter. The cell was filmed at 0.5 fps for a total of 118 s. The movie is accelerated 20x.

Supplemental Movie 5

Higher magnification detail of the 60 frame-sequence of Sec13-mCherry and CopA-GFP shown in Movie 4.

ACCEPTED MANUSCRIPT

ACCEPTED MANUSCRIPT

References

Arst, H. N., Jr., et al., 2014. GBF/Gea mutant with a single substitution sustains fungal growth in the absence of BIG/Sec7. FEBS Lett. 588**,** 4799-4786.

Barlowe, C. K., Miller, E. A., 2013. Secretory protein biogenesis and traffic in the early secretory pathway. Genetics. 193**,** 383-410.

Béraud-Dufour, S., et al., 1999. Dual Interaction of ADP ribosylation factor 1 with Sec7 domain and with lipid membranes during catalysis of guanine nucleotide exchange. Journal of Biological Chemistry. 274**,** 37629-37636.

Breakspear, A., et al., 2007. CopA:GFP localizes to putative Golgi equivalents in *Aspergillus nidulans*. FEMS Microbiology Letters. 277**,** 90-97.

Cove, D. J., 1966. The induction and repression of nitrate reductase in the fungus *Aspergillus nidulans.* Biochimica and Biophysica Acta. 113**,** 51-56.

Daboussi, L., et al., 2012. Phosphoinositide-mediated clathrin adaptor progression at the trans-Golgi network. Nature Cell Biology. 14**,** 239-48.

Day, K. J., et al., 2013. A three-stage model of Golgi structure and function. Histochem Cell Biol. 140**,** 239-49.

Dodonova, S. O., et al., 2017. 9Å structure of the COPI coat reveals that the Arf1 GTPase occupies two contrasting molecular environments. eLife. 6**,** e26691.

Dodonova, S. O., et al., 2015. VESICULAR TRANSPORT. A structure of the COPI coat and the role of coat proteins in membrane vesicle assembly. Science. 349**,** 195-8.

Eugster, A., et al., 2004. The alpha- and beta'-COP WD40 domains mediate cargo-selective interactions with distinct di-lysine motifs. Mol Biol Cell. 15**,** 1011-23.

Glick, B. S., Luini, A., 2011. Models for Golgi traffic: a critical assessment. Cold Spring Harbour Perspectives in Biology. 3**,** a005215.

Glick, B. S., Nakano, A., 2009. Membrane traffic within the Golgi apparatus. Annual Review of Cellular and Developmental Biology. 25**,** 113-132.

Gommel, D. U., et al., 2001. Recruitment to Golgi membranes of ADP‐ribosylation factor 1 is mediated by the cytoplasmic domain of p23. The EMBO Journal. 20**,** 6751-6760.

Hara-Kuge, S., et al., 1994. En bloc incorporation of coatomer subunits during the assembly of COP-coated vesicles. J Cell Biol. 124**,** 883-92.

Hernández-González, M., et al., 2018. Genetic dissection of the secretory route followed by a fungal extracellular glycosyl hydrolase. Molecular Microbiology. 109**,** 781-800.

Hernández-González, M., et al., 2014. Conditional inactivation of *Aspergillus nidulans sarA* uncovers the morphogenetic potential of regulating endoplasmic reticulum (ER) exit. Mol Microbiol. 95**,** 491-508.

Hsia, K. C., Hoelz, A., 2010. Crystal structure of alpha-COP in complex with epsilon-COP provides insight into the architecture of the COPI vesicular coat. Proc Natl Acad Sci U S A. 107**,** 11271-6.

Kall, L., et al., 2007. Semi-supervised learning for peptide identification from shotgun proteomics datasets. Nat Methods. 4**,** 923-5.

Kang, E. H., et al., 2015. Depletion of epsilon-COP in the COPI Vesicular Coat Reduces Cleistothecium Production in Aspergillus nidulans. Mycobiology. 43**,** 31-6.

Kurokawa, K., et al., 2014. Contact of cis-Golgi with ER exit sites executes cargo capture and delivery from the ER. Nat Commun. 5**,** 3653.

Lee, H. H., et al., 2002. Aspergillus nidulans sod(VI)C1 mutation causes defects in cell wall biogenesis and protein secretion. FEMS Microbiol Lett. 208**,** 253-7.

ACCEPTED MANUSCRIPT

Levine, T. P., Munro, S., 2002. Targeting of Golgi-specific pleckstrin homology domains involves both PtdIns 4-kinase-dependent and -independent components. Current Biology. 12**,** 695-704.

Liu, H. L., et al., 2010. Single-step affinity purification for fungal proteomics. Eukaryot Cell. 9**,** 831-3.

López-Berges, M. S., et al., 2016. The *Aspergillus nidulans* syntaxin PepA is regulated by two Sec1/Munc-18 proteins to mediate fusion events at early endosomes, late endosomes and vacuoles. Mol Microbiol. 99**,** 199-216.

Losev, E., et al., 2006. Golgi maturation visualized in living yeast. Nature. 441**,** 1002-1006.

Martzoukou, O., et al., 2018. Secretory vesicle polar sorting, endosome recycling and cytoskeleton organization require the AP-1 complex in *Aspergillus nidulans*. Genetics. 209**,** 1121-1138.

Matsuura-Tokita, K., et al., 2006. Live imaging of yeast Golgi cisternal maturation. Nature. 441**,** 1007-1010.

Mossessova, E., et al., 2003. Crystal structure of ARF1*Sec7 complexed with Brefeldin A and its implications for the guanine nucleotide exchange mechanism. Molecular Cell. 12**,** 1403-11.

Pantazopoulou, A., 2016. The Golgi apparatus: insights from filamentous fungi. Mycologia. 108**,** 603-622.

Pantazopoulou, A., Peñalva, M. A., 2009. Organization and dynamics of the *Aspergillus nidulans* Golgi during apical extension and mitosis. Molecular Biology of the Cell. 20**,** 4335-4347.

Pantazopoulou, A., Peñalva, M. A., 2011. Characterization of *Aspergillus nidulans* RabC^{Rab6}. Traffic. 12**,** 386-406.

Pantazopoulou, A., et al., 2014. Maturation of late Golgi cisternae into RabE^{RAB11} exocytic post-Golgi carriers visualized *in vivo*. Molecular Biology of the Cell. 25**,** 2428-2443.

Papanikou, E., et al., 2015. COPI selectively drives maturation of the early Golgi. eLife.

Papanikou, E., Glick, B. S., 2014. Golgi compartmentation and identity. Curr Opin Cell Biol. 29C**,** 74-81.

Peñalva, M. A., et al., 2017. Transport of fungal RAB11 secretory vesicles involves myosin-5, dynein/dynactin/p25 and kinesin-1 and is independent of kinesin-3. Molecular Biology of the Cell. 28**,** 947-961.

Peyroche, A., et al., 1999. Brefeldin A acts to stabilize an abortive ARF-GDP-Sec7 domain protein complex: involvement of specific residues of the Sec7 domain. Molecular Cell. 3**,** 275-285.

Pinar, M., et al., 2015. TRAPPII regulates exocytic Golgi exit by mediating nucleotide exchange on the Ypt31 orthologue RabE/RAB11. Proceedings of the National Academy of Sciences USA. 112**,** 4346-4351.

Pinar, M., et al., 2013a. Acute inactivation of the *Aspergillus nidulans* Golgi membrane fusion machinery: correlation of apical extension arrest and tip swelling with cisternal disorganization. Molecular Microbiology. 89**,** 228-248.

Pinar, M., et al., 2013b. Live-cell imaging of *Aspergillus nidulans* autophagy: RAB1 dependence, Golgi independence and ER involvement. Autophagy. 9**,** 1024-1043.

Rabouille, C., Klumperman, J., 2005. Opinion: The maturing role of COPI vesicles in intra-Golgi transport. Nat.Rev.Mol.Cell.Biol. 6**,** 812-817.

Renault, L., et al., 2003. Structural snapshots of the mechanism and inhibition of a guanine nucleotide exchange factor. Nature. 426**,** 525-30.

Rossanese, O. W., et al., 1999. Golgi structure correlates with transitional endoplasmic reticulum organization in *Pichia pastoris* and *Saccharomyces cerevisiae*. Journal of Cell Biology. 145**,** 69-81.

ACCEPTED MANUSCRIPT

Schroder-Kohne, S., et al., 1998. Alpha-COP can discriminate between distinct, functional di-lysine signals in vitro and regulates access into retrograde transport. J Cell Sci. 111 (Pt 23), 3459-70.

Schultzhaus, Z., et al., 2017. Clathrin localization and dynamics in *Aspergillus nidulans*. Molecular Microbiology. 103, 299-318.

Spang, A., 2013. Traffic COPs: rules of detection. EMBO J. 32, 915-6.

Sprangers, J., Rabouille, C., 2015. SEC16 in COPII coat dynamics at ER exit sites. Biochem Soc Trans. 43, 97-103.

Szewczyk, E., et al., 2006. Fusion PCR and gene targeting in *Aspergillus nidulans*. Nat Protoc. 1, 3111-20.

Upshall, A., Mortimore, I. D., 1984. Isolation of aneuploid-generating mutants of Aspergillus nidulans, one of which is defective in interphase of the cell cycle. Genetics. 108, 107-21.

Whittaker, S. L., et al., 1999. *sodVIC* Is an alpha-COP-related gene which Is essential for establishing and maintaining polarized growth in *Aspergillus nidulans* Fungal Genetics and Biology. 26, 236-252.

Wooding, S., Pelham, H. R. B., 1998. The dynamics of Golgi protein traffic visualized in living yeast cells. Molecular Biology of the Cell. 9, 2667-2680.

Yang, J. S., et al., 2011. COPI acts in both vesicular and tubular transport. Nature Cell Biology. 13, 996-1003.

Yu, X., et al., 2012. A structure-based mechanism for Arf1-dependent recruitment of coatomer to membranes. Cell. 148, 530-42.

ACCEPTED MANUSCRIPT

ACCEPTED MANUSCRIPT

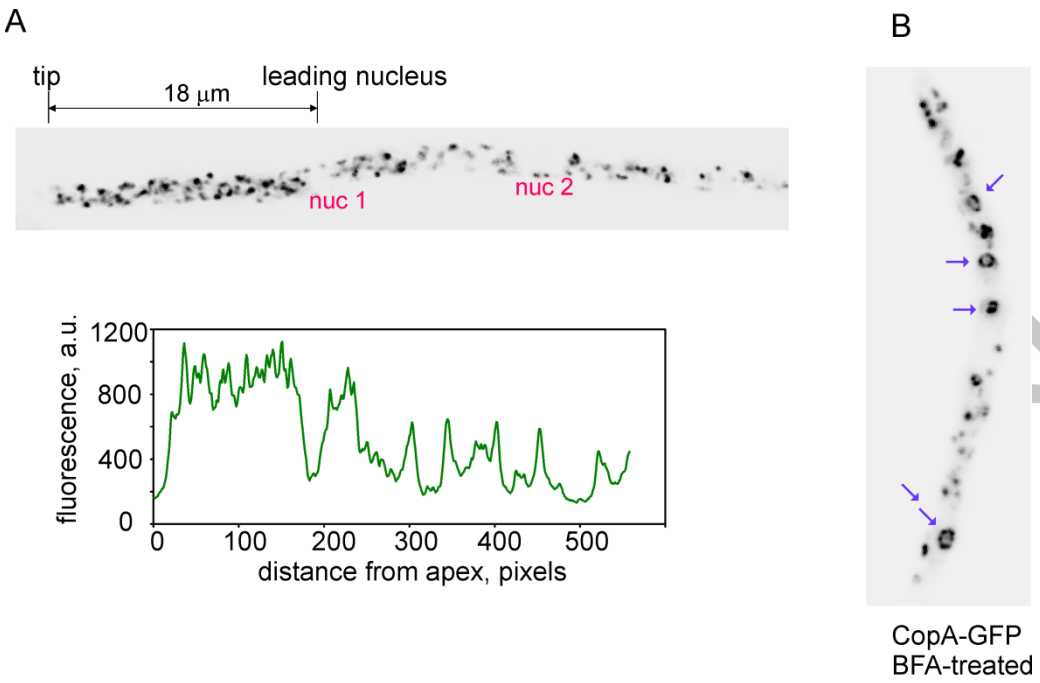

Figure 1, Hernández-González et al

ACCEPTED MANUSCRIPT

ACCEPTED MANUSCRIPT

gene	subunit	aa no.	PSMs CopA-S	PSMs mock	score
AN3026	α-COP	1211	705	12	582
AN5972	β-COP	853	441	10	517
AN1117	β'-COP	950	330	4	347
AN0922	δ-COP	516	132	0	256
AN0665	ε-COP	296	52	1	176
AN4547	γ-COP	917	72	0	79
AN6080	ζ-COP	200	6	1	30

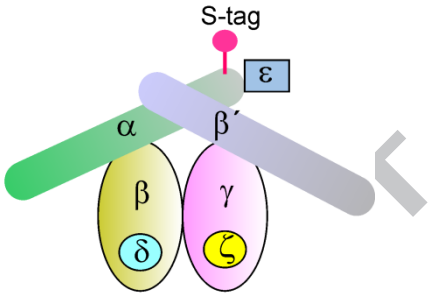

α
β' outer coat subcomplex
ε

β
δ adaptor subcomplex
γ
ζ

Figure 2, Hernández-González et al

ACCEPTED MAN

ACCEPTED MANUSCRIPT

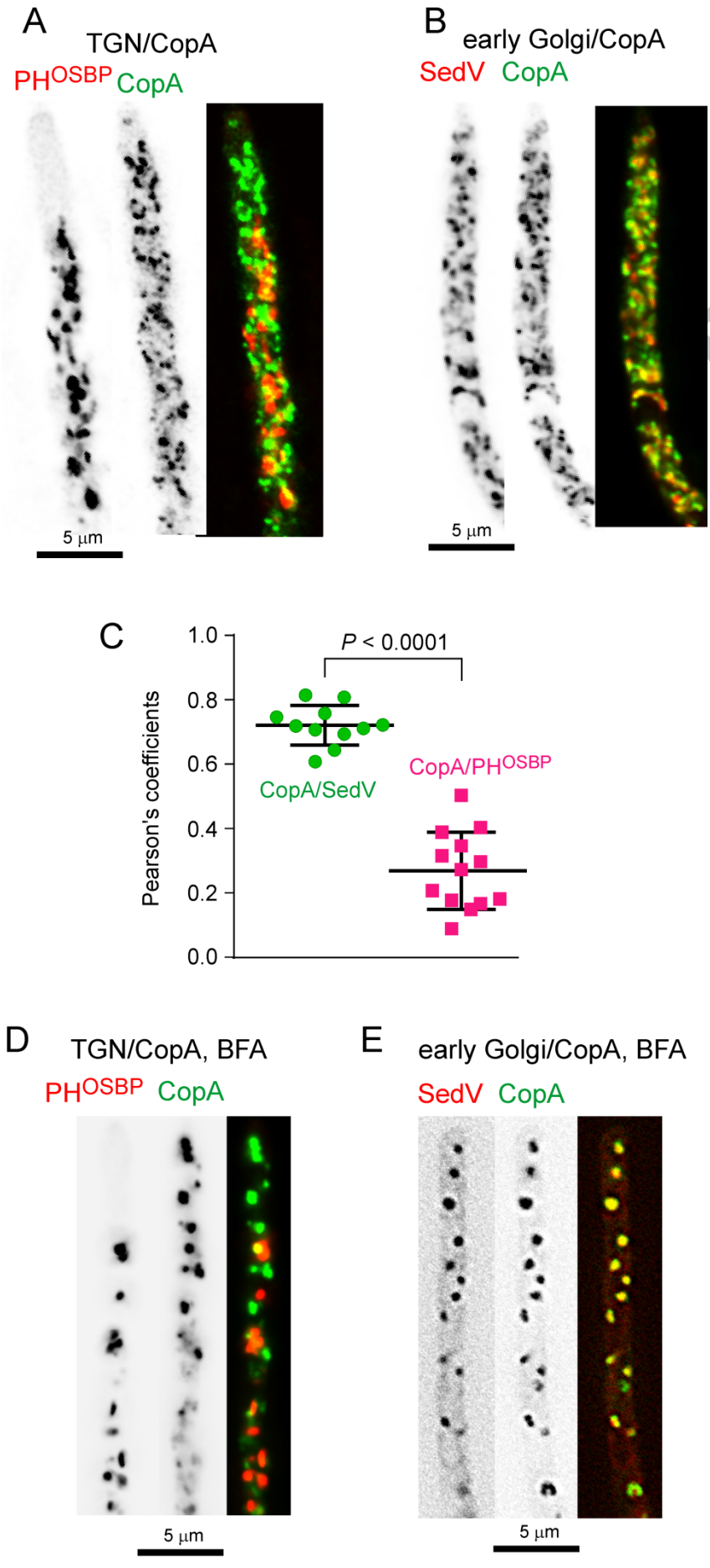

Figure 3, Hernández-González et al

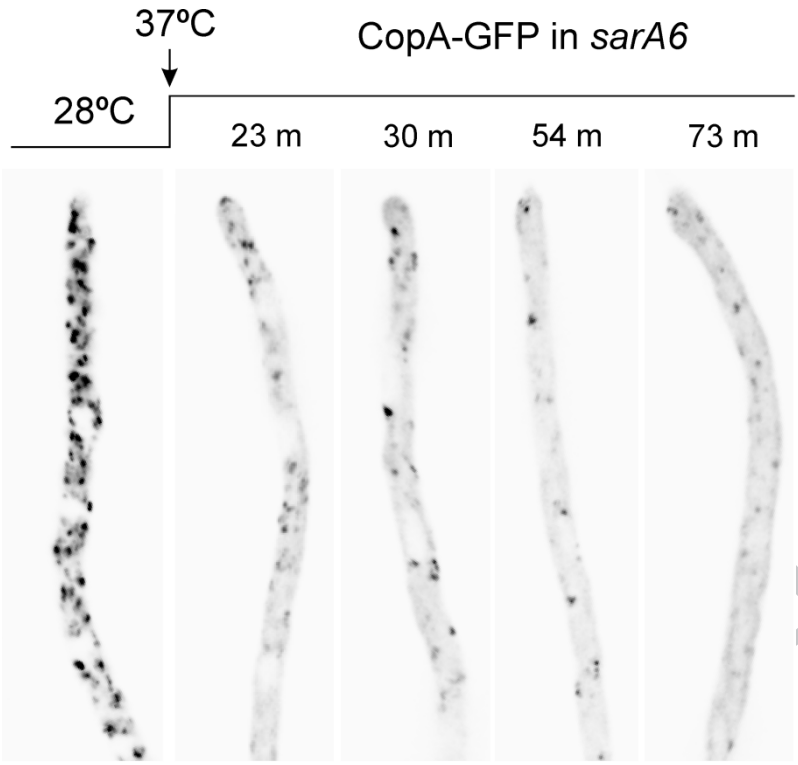

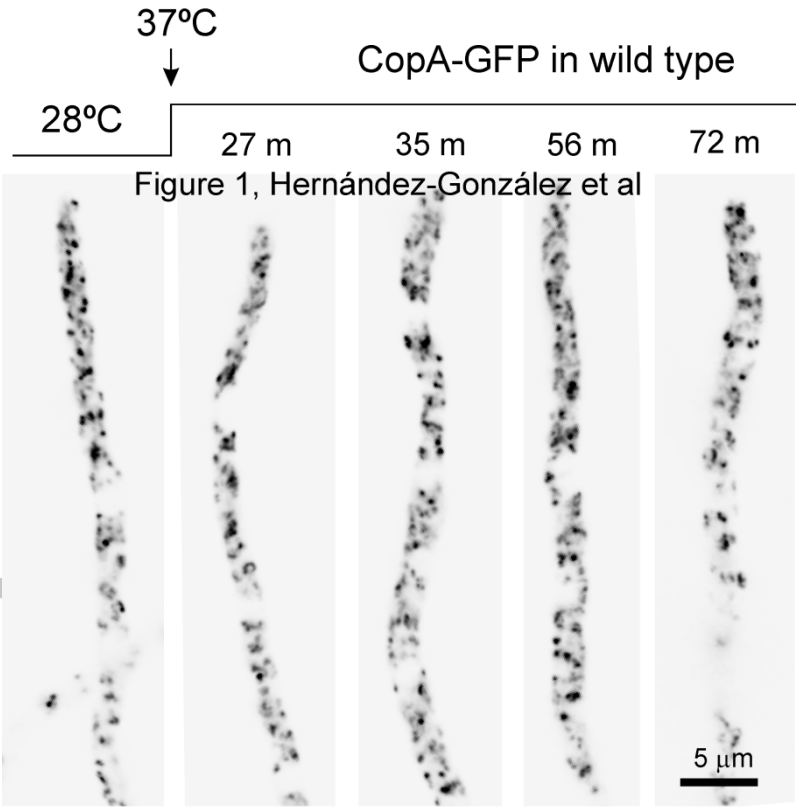

Figure 1, Hernández-González et al

Figure 4, Hernández-González et al

ACCEPTED MANUSCRIPT

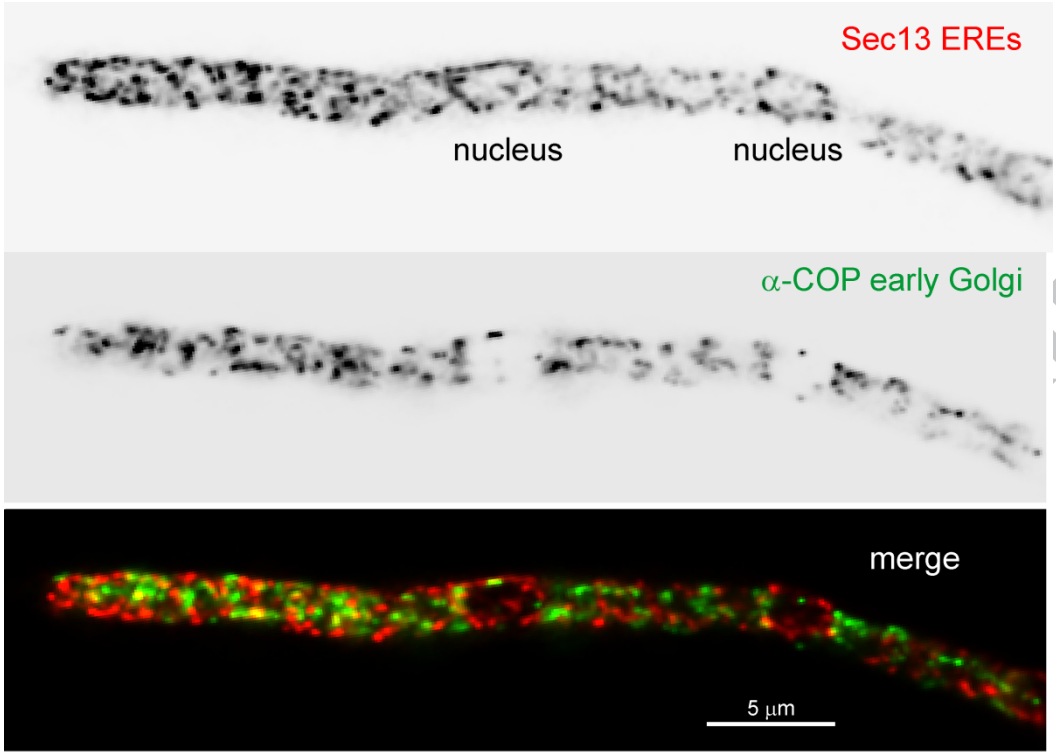

Figure 5, Hernández-González et al

ACCEPTED MANUSCRIPT

ACCEPTED MANUSCRIPT

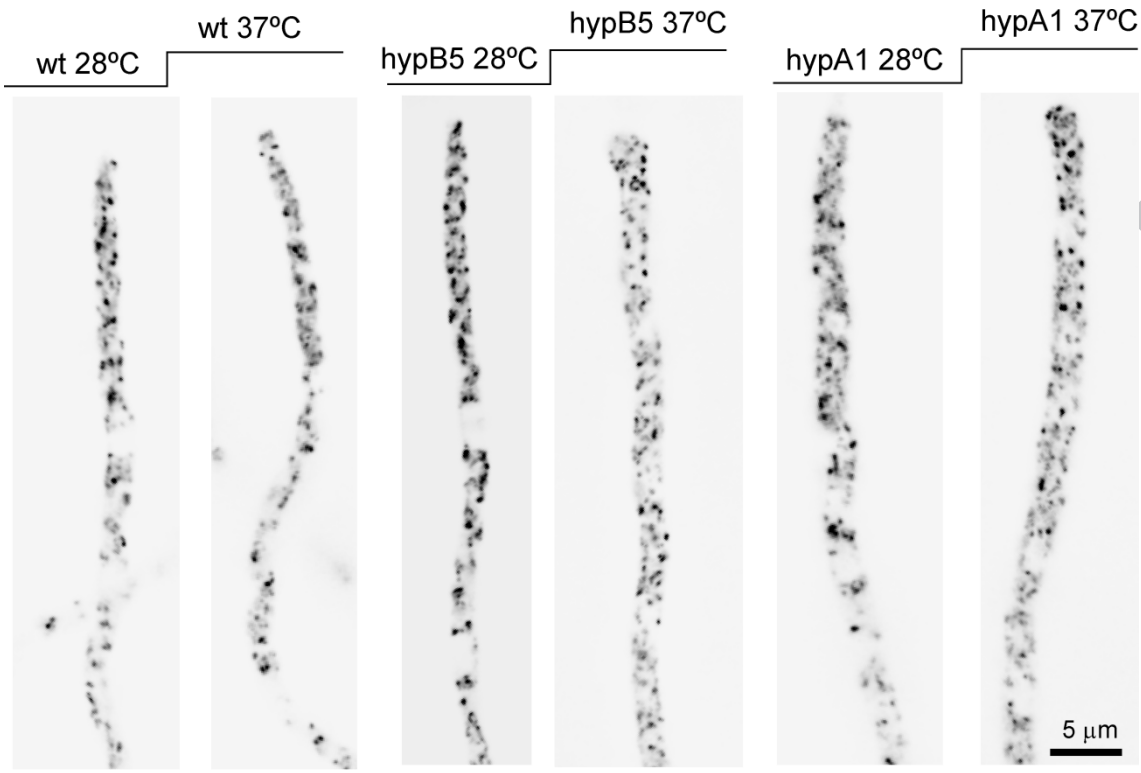

CopA-GFP localization

Figure 6, Hernández-González et al

ACCEPTED

ACCEPTED MANUSCRIPT

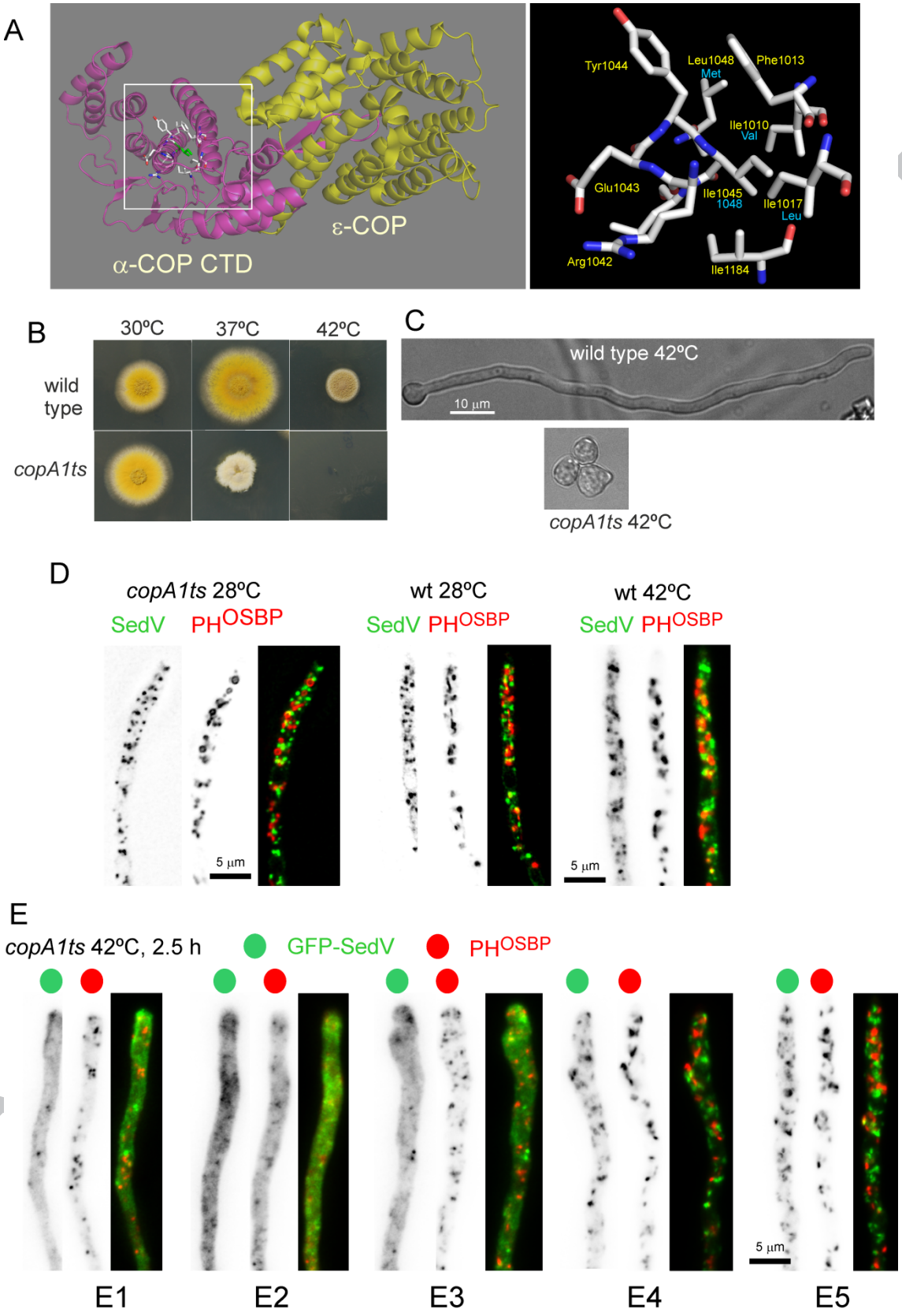

Figure 7, Hernández-González et al

ACCEPTED MANUSCRIPT

Table I. Strains used in this work

MAD Strain no.	Genotype
1739	*pyrG*89; *pyroA*4 *nkuAΔ::bar*
3331	*argB2::[argB*-gpdA^{m}::GFP-sedV]; inoB2 pyroA4::[pyroA*-gpdA^{m}::mRFP-PH^{OSBP}]; pantoB100,*
3797	*pabaA1 yA2; argB2::[argB*-gpdA^{m}::GFP-sedV]; pyroA4::[pyroA*-gpdA^{m}::mRFP-PH^{OSBP}]; copA1ts; pantoB100*
3798	*pabaA1 yA2; argB2::[argB*-gpdA^{m}::GFP-sedV]; pyroA4::[pyroA*-gpdA^{m}::mRFP-PH^{OSBP}]; copA1ts*
3822	*pabaA1 yA2, copA1ts*
4503	*pyrG*89; *pyroA*4 *nkuAΔ::bar*; *copA-GFP::pyrG*^{Af}
4601	*pyrG*89? *hypB*5; *pyroA*4 *nkuAΔ::bar*?; *copA-GFP::pyrG*^{Af}
4602	*pyrG89?; wA4; pyroA4::[pyroA*-gpdA^{m}::mRFP-PH^{OSBP}] nkuAΔ::bar?; copA-GFP::pyrG^{Af}; niiA4*
4605	*pyrG89?; pyroA4::[pyroA*-gpdA^{m}::mCherry-sedV] ΔnkuA::bar inoB2; copA-GFP::pyrG^{Af}*
4982	*pyrG89?; pyroA4 nkuAΔ::bar inoB2; copA-GFP::pyrG^{Af}; sarA6::pyrG^{Af}*
5319	*pyrG89*; *pyroA4 nkuAΔ::bar*; *riboB2*
6126	*pyrG89*; *sec13-mCherry::pyrG^{Af}*; *pyroA4 nkuAΔ::bar*
6202	*hypA1; wA3; pyroA4 nkuAΔ::bar; copA-GFP::pyrG^{Af}*
6289	*pyrG*89?; *sec13-mCherry::pyrG^{Af}*; *pyroA*4 *nkuAΔ::bar*?; *copA-GFP::pyrG^{Af}*
6765	*pyrG89 pyroA*4 *nkuAΔ::bar*; *copA-S-tag::pyrG^{Af}*; *riboB*2

ACCEPTED MANUSCRIPT